

## Article

# Response of Vegetation Dynamics in the Three-North Region of China to Climate and Human Activities from 1982 to 2018

Weijia Liang, Quan Quan \*, Bohua Wu and Shuhong Mo

State Key Laboratory of Eco-Hydraulics in Northwest Arid Region, Xi'an University of Technology, Xi'an 710048, China

\* Correspondence: qq@xaut.edu.cn

**Abstract:** To tackle ecological problems, many ecological restoration projects have been implemented in northern China. Identifying the drivers of vegetation change is critical for continued ecological engineering. In this study, three typical ecological reserves in the Three-North Shelter Forest Program Region (TNSFR) were selected to identify their vegetation development characteristics and driving mechanisms using the normalized difference vegetation index (NDVI), climate factors, and land use data. The results show that (1) NDVIs increased in the range of human activities of all of the three ecological reserves, indicating an obvious effect of the vegetation restoration projects. (2) In the planting period, vegetation restoration was mainly correlated with human activities. After entering the tending period, the impact of climate changes on vegetation dynamics was enhanced. (3) Temperature and precipitation provided approximate driving effects on vegetation dynamics in Region I, while vegetation dynamics in Regions II and III were more strongly correlated with precipitation. (4) The proportion of areas with ecological measures exceeded 50% in all three regions. In short, ecological projects in the three ecological reserves dominated the quantity of vegetation restoration, while climate changes influenced the quality of vegetation restoration.

**Keywords:** vegetation dynamics; climate factors; human intervention; national key ecology project; ecological restoration



**Citation:** Liang, W.; Quan, Q.; Wu, B.; Mo, S. Response of Vegetation Dynamics in the Three-North Region of China to Climate and Human Activities from 1982 to 2018. *Sustainability* **2023**, *15*, 3073. <https://doi.org/10.3390/su15043073>

Academic Editor: Adriano Stinca

Received: 30 December 2022

Revised: 1 February 2023

Accepted: 5 February 2023

Published: 8 February 2023



**Copyright:** © 2023 by the authors. Licensee MDPI, Basel, Switzerland. This article is an open access article distributed under the terms and conditions of the Creative Commons Attribution (CC BY) license (<https://creativecommons.org/licenses/by/4.0/>).

## 1. Introduction

Vegetation is the manifestation of the ecological environment and a crucial factor in the development of a ground landscape system [1,2]. It not only takes part in the land–atmosphere energy cycle and coupled carbon–water cycle but also is an important component in ecological projects to curb desertification and conserve water and soil [3,4]. Existing research considers that vegetation dynamics are under the dual action of climate conditions and human activities [5,6]. Therefore, it is very important to study the response of vegetation dynamics to climate change and human activities for evaluating the implementation effects of ecological projects. However, it is necessary to select an appropriate vegetation index to reflect vegetation dynamics. The normalized difference vegetation index (NDVI) can reflect the growth status of plants [7]. NDVIs are widely applied to monitor vegetation dynamics due to their wide coverage, long data collection time, and high observation accuracy [8–10].

Vegetation dynamics directly reflect the implementation effect of ecological restoration projects, so identifying driving mechanisms of vegetation dynamics is significant for the continuous implementation of ecological projects. With the background of the increasingly clear impact of climate changes, quantifying the relative contributions of climate changes and human activities to vegetation dynamics has become a critical link in identifying the driving mechanisms of vegetation dynamics. Plenty of relevant studies on quantifying vegetation drivers have been conducted [11–13]. The commonly used methods include the regression model, geographical detector model, and biophysical model. Therein, residual

trend analysis (Restrend) constructs fitting equations based on meteorological factors to simulate vegetation indices. Then, the change trends of the simulated and measured values are compared, and the impacts of human activities on vegetation are separated, so as to assess the relative effects of climate changes and human activities on vegetation dynamics. Restrend has become a common method to quantify the impacts of climate changes and human activities on vegetation due to its convenience and universality [14,15].

Previous studies have determined that meteorological factors such as temperature and precipitation are the controlling factors of global vegetation change, and human activities such as agriculture and urbanization also have an impact on vegetation dynamics [16–19].

The Three-North Shelterbelt Project has been carried out for many years. Existing research shows that the greening effect of vegetation in the TNSFR is smaller than that in other ecological project areas, which may be limited by water resources [20,21]. However, the TNSFR covers a vast area, and the research is mostly carried out within the whole project area [21,22]. It needs to be divided into sub-regions for deep research to obtain a more accurate dynamic driving force of vegetation.

The aim of ecological engineering is to restore vegetation and improve the ecological environment. However, due to the impact of various factors on the vegetation dynamics, the effect of the ecological restoration project is different from the expected. It is necessary to determine the effect of ecological engineering in a changing environment. Therefore, the purposes of this study are as follows: (1) analyze the spatiotemporal distribution of vegetation in the ecological reserves; (2) quantify the relative contributions of climate changes and human activities to vegetation dynamics; and (3) explore the driving mechanisms of climate factors and human activities for vegetation dynamics. Based on vegetation conditions in different ecological reserves, the research intended to evaluate the implementation effect of the ecological restoration project and provide a scientific basis for strategy formulation on the basis of maintaining the implementation effects of existing ecological projects, further enhancing the ecological benefits, and realizing the harmonious coexistence of humans and nature.

## 2. Materials and Methods

The complete framework of this study is shown in Figure 1. First of all, this paper analyzes the spatiotemporal characteristics of the NDVI to identify the vegetation dynamics with change-point analysis and linear trend analysis. Then, the impacts of human activities and climate changes on vegetation dynamics are separated based on the residual method to quantify their individual contributions to vegetation dynamics. Finally, the driving effects of climate changes and human activities on vegetation dynamics are explored separately. The impact of climate changes on vegetation is analyzed by calculating partial correlations of climate factors such as temperature and precipitation with the NDVI. Using land cover data, the intensity index and the land-use type matrix are established to analyze the impact of human activities on vegetation.

### 2.1. Overview of Research Areas

To deal with ecological problems, the Three-North Shelter Forest Program has been implemented in China since 1978 to build a green barrier by planting vegetation so as to restore regional ecological functions [23–25]. The TNSFR refers to the large-scale artificial forestry project carried out in northeastern, northern, and northwestern China and covers 13 provincial-level administrative regions (73°–130° E, 33°–50° N). Multiple ecological restoration projects in the Three-North Shelter Forest Program Region (TNSFR) have been implemented to improve and protect local vegetation [26–29]. Information on the main ecological projects is summarized in Table 1.

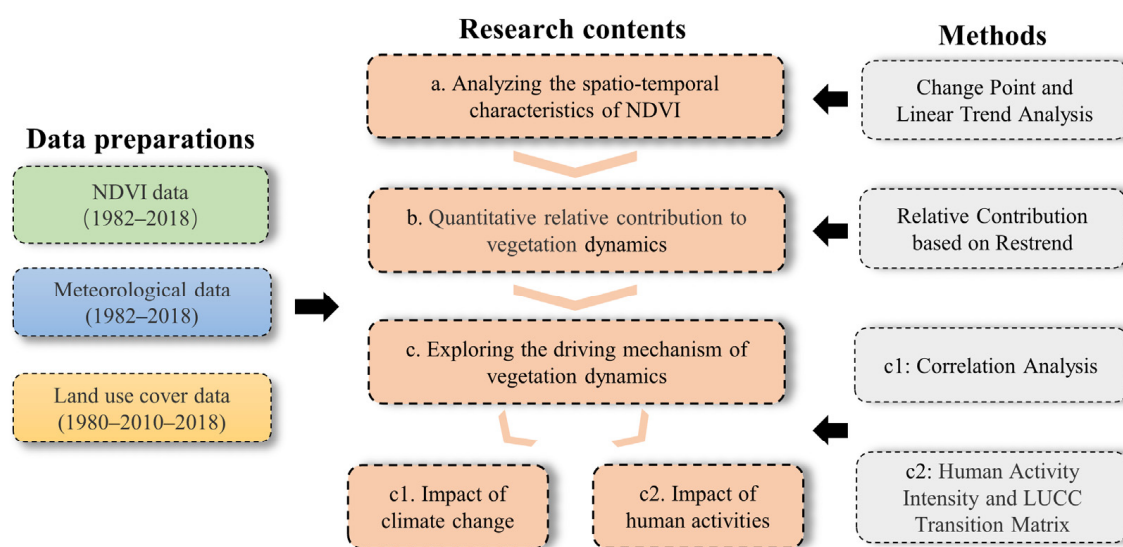


**Figure 1.** Research framework of this study.

**Table 1.** Summary of ecological projects in the TNSFR.

Ecological Projects	Initial Time	Area Affected	Aims
1. Three-North Shelter Forest Program	1978	13 provinces in northern, northwestern, and northeastern China	Curb desertification and prevent soil erosion
2. Shelterbelt Construction for Cropland Project	1987	Northern and northeastern China	Resist desertification and protect cropland
3. Natural Forest Protection Program	1998	Western China	Conserve key natural ecosystems
4. Restoring Cropland to Forest Program	1999	Western China	Restrain soil erosion and increase vegetation coverage
5. Sand Source Controls Project	2000	5 provinces around Beijing	Control land and protect vegetation

The region spans a large geographical range from the eastern coastal areas to the north-west inland, which features complex underlying surface conditions and meteorological conditions. According to the geographical conditions and climate conditions of the TNSFR, the Tarim River Basin Ecological Reserve (Region I), Loess Plateau Ecological Reserve (Region II), and Beijing-Tianjin Sand Source Control Region (Region III) in the region were selected as representative regions. The spatial distribution of the three ecological reserves is illustrated in Figure 2.

In the three study areas, the main form of vegetation restoration activities is afforestation and grass planting. The Three-North Shelterbelt Project has a long period. In the early stage of project implementation, large-scale vegetation planting is often the main focus and is called the planting period; as the project continues, vegetation tending becomes the focus of work and is called the tending period.

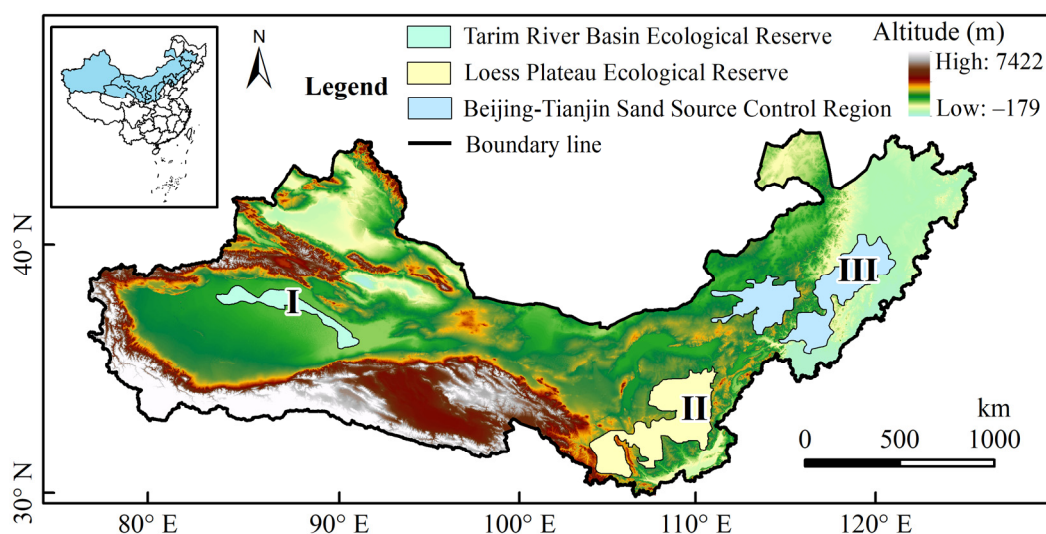


**Figure 2.** Research regions. Region I (Tarim River Basin Ecological Reserve); Region II (Loess Plateau Ecological Reserve); and Region III (Beijing-Tianjin Sand Source Control Region).

## 2.2. Data Collection and Processing

The NDVI data used in the research were derived from MOD13A3 datasets and GIMMS datasets [30]. Meteorological data including temperature and precipitation came from the CMFD dataset [31,32]. The boundaries of ecological reserves and land-use type data were collected from the Resource and Environment Science and Data Center. Because of the absence of land-use type data in 1982, those in 1980 were used to replace the land-use types in 1982. Table 2 displays detailed information on the data used in this research.

**Table 2.** Data sources and detailed information.

Data Type	Data Name	Data Source	Spatial Resolution	Time Resolution	Length of Time
NDVI	GIMMS	National Tibetan Plateau Data Center	8 km	Month	1982–2015
	MOD13A3	LAADS DAAC	1 km	Month	2016–2018
Temperature and precipitation	CMFD	National Tibetan Plateau Data Center	0.1°	Year	1982–2018
Land-use type	LUCC	Resource and Environment Science and Data Center	1 km	Year	1980, 2010, 2018

The time length of the GIMMS dataset is in the range of 1982–2015. To ensure consistency in an NDVI series and meteorological data, the time of the NDVI data needs to be prolonged to 2018 by combining with another NDVI dataset. Existing research shows that GIMMS data are highly correlated with MODIS data, so MODIS data were adopted to prolong the GIMMS dataset [33–35]. Because of the lowest spatial resolution of CMFD data, NDVI data should be normalized to the resolution of CMFD data for the convenience of analysis, as shown below.

## 2.3. Methods

### 2.3.1. Annual Maximum Method

Because the NDVI is observed by using remote sensing satellites, the observation quality is interfered with by many factors. The annual maximum method is commonly used to reduce the influences of cloud and water vapor on NDVI observation values [36]. The calculation formula is as follows:

$$NDVI_i = \max(NDVI_j) \quad (1)$$

where  $NDVI_i$  represents the NDVI value in the  $i$ th year and  $NDVI_j$  is the NDVI value in the  $j$ th month of the  $i$ th year, and  $j$  is valued in the range of 1–12.

### 2.3.2. Heuristic Segmentation Algorithm

The heuristic segmentation algorithm is commonly used to calculate points with abrupt changes in a non-stationary series [37]. By calculating the pooled deviation at each point in the test series, the T statistical values are established, and statistical significance  $p(T_{\max})$  corresponding to  $T_{\max}$  is calculated. A critical value  $P_0$  is set. If  $p(T_{\max}) > p_0$ , the test series is segmented into two sub-series at that point; otherwise, the series is not segmented. Herein, the critical value is set to 0.95. The above operation is repeated until the length of the sub-series is shorter than or equal to  $l_0$  (the minimum segmentation scale is valued to 25) when the segmentation stops. Under this condition, the segmentation point is the point with abrupt changes in the testing series [38].

According to the year of abrupt changes, the research period is divided into two time intervals. The time interval before the year of abrupt changes is the planting period, while that after the year is the tending period.

### 2.3.3. Linear Trend Analysis

Trend analysis at the pixel scale can better reflect the development trend in the study area. The linear regression equation can be used to evaluate the trend of the NDVI at the pixel scale. [39]

$$\theta_{slope} = \frac{N \times \sum_{i=1}^N i \times NDVI - \sum_{i=1}^N i \sum_{i=1}^N NDVI_i}{N \times \sum_{i=1}^N i^2 - (\sum_{i=1}^N i)^2} \quad (2)$$

where  $\theta_{slope}$  is the slope of the linear regression equation, which can represent the change in NDVI during the research period. When  $\theta_{slope} > 0$ , this shows that the NDVI has an upward trend, and when  $\theta_{slope} < 0$ , the NDVI has a downward trend.  $N$  is the total number of years, and  $I$  represents the serial number of the year. The F test ( $p < 0.05$ ) is used for the significance test. If the significance test is passed, this indicates that the change trend of NDVI is significant.

### 2.3.4. Calculating Contributions Based on the Residual Method

The residual analysis method is commonly used to calculate the relative contributions of climate changes and human activities [40,41]. At first, a multiple linear regression equation is constructed based on climate factors to predict the NDVIs only affected by climate change. By analyzing the trends of measured NDVIs, NDVIs only affected by climate changes, NDVIs only affected by human activities, and the relative contributions of climate changes and human activities to vegetation development are quantified [42,43]. The NDVI values only impacted by human activities are calculated as follows [44,45]:

$$NDVI_c = aT + bP + c \quad (3)$$

$$\varepsilon_i = NDVI_i - NDVI_{ci} \quad (4)$$

where  $NDVI_c$  is the simulated value of the multiple linear regression equation built based on climate factors;  $a$ ,  $b$ , and  $c$  are regression coefficients of temperature, precipitation, and a constant term;  $\varepsilon_i$  is the residual between the measured NDVI and simulated NDVI in the  $i$ th year;  $\varepsilon_i > 0$  and  $\varepsilon_i < 0$  separately indicate that human activities promote vegetation improvement and vegetation degradation;  $NDVI_i$  denotes the measured value in the  $i$ th year; and  $NDVI_{ci}$  is a fitted value based on the impact of climate changes in the  $i$ th year.

The driving effects are divided into the human-activity-dominated (HA), the climate change-dominated (CC), and both factors combined (BC) [46]. The three driving effects are further divided into vegetation restoration (HAR, CCR, and BCR) and vegetation degradation (HAD, CCD, and BCD) according to vegetation changes. The types of driving mechanisms of vegetation dynamics are listed in Table 3.

**Table 3.** Evaluation methods for dominated driving factors of vegetation dynamics.

Vegetation Dynamics	Judgment Conditions		Driving Mechanisms of Vegetation Dynamics
	$Slope_O$	$Slope_H$ and $Slope_C$	
Vegetation degradation	$Slope_O < 0$	$Slope_H > 0, Slope_C < 0$	
		$Slope_H < 0, Slope_C < 0$ $Slope_H < 0, Slope_C > 0$ $Slope_H < 0, Slope_C > 0$	
$Slope_O > 0$	$Slope_H > 0, Slope_C > 0$		
	$Slope_H > 0, Slope_C < 0$		

Notes:  $Slope_O$ : slope of the measured NDVI;  $Slope_C$  and  $Slope_H$ : slopes of NDVIs only impacted by climate changes and human activities, respectively.

2.3.5. Partial Correlation Analysis Method

When a certain variable is influenced by multiple factors, it is generally necessary to perform a partial correlation analysis to eliminate the influences of other variables so as to acquire correlations between two factors [47]. In this research, the partial correlation coefficient was adopted to investigate the influences of temperature and precipitation on the variation in the NDVI [48,49].

$$r_{xy,z} = \frac{r_{xy} - r_{xz}r_{yz}}{\sqrt{(1 - r_{xz}^2)(1 - r_{yz}^2)}} \tag{5}$$

where  $r_{xy,z}$  denotes the first-order partial correlation coefficient between  $x$  and  $y$  after eliminating their influences of factor  $z$ .  $r_{xy}$ ,  $r_{xz}$ , and  $r_{yz}$  represent the correlation coefficients between  $x$  and  $y$ , between  $x$  and  $z$ , and between  $y$  and  $z$ , respectively.

2.3.6. Human Activity Intensity

Human activity intensity can be used to characterize land cover use of humans in a region. According to different degrees of utilization for different ecological systems, different conversion coefficients are assigned to finally calculate the human activity intensity with the following formula [50]:

$$HAI = \frac{\sum_{i=1}^N (SL_i \times CI_i)}{S} \times 100\% \tag{6}$$

where  $HAI$  denotes the human activity intensity;  $S$  is the total area of the region;  $SL_i$  denotes the area of the  $i$ th land cover type; and  $CI_i$  is the conversion coefficient of the  $i$ th land cover type. The conversion coefficients of different land cover types are listed in Table 4.

**Table 4.** Conversion coefficients of different land-use/cover types.

Land-Use Type	Unused Land	Forest and Grassland	Cropland	Water	Urban
CI	0	0.133	0.2	0.6	1

According to dynamic changes in land cover types, human activities are classified into ecological measures and development activities. The former mainly includes afforestation and grass planting, while the latter mainly includes agricultural reclamation and urban expansion [51].

### 2.3.7. Land-use Transition Matrix

The land-use transition matrix is commonly adopted to describe the transition and changes in each land-use type in a certain period. It reflects the area and direction of the transition in each land-use type [52,53]. The land-use transition matrix is expressed by the following equation:

$$A_{ij} = \begin{bmatrix} A_{11} & \cdots & A_{1n} \\ \vdots & \ddots & \vdots \\ A_{n1} & \cdots & A_{nn} \end{bmatrix} \quad (7)$$

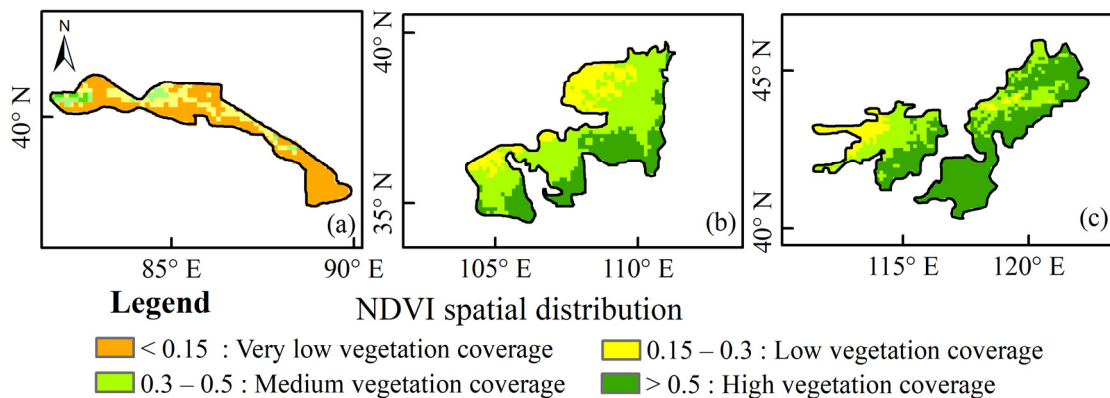
where  $A_{ij}$  denotes the area of the  $i$ th land-use type transformed into the  $j$ th type, in which  $i$  is the initial land-use type and  $j$  is the land-use type at the end of the research. Moreover,  $n$  refers to the number of land-use types, and  $n$  is valued to be 6 in this research, including cropland, forest, grassland, unused land, urban, and water.

## 3. Results

### 3.1. Temporal and Spatial Changes in NDVIs in Typical Ecological Reserves in 1982–2018

#### 3.1.1. Spatial Characteristics of NDVIs

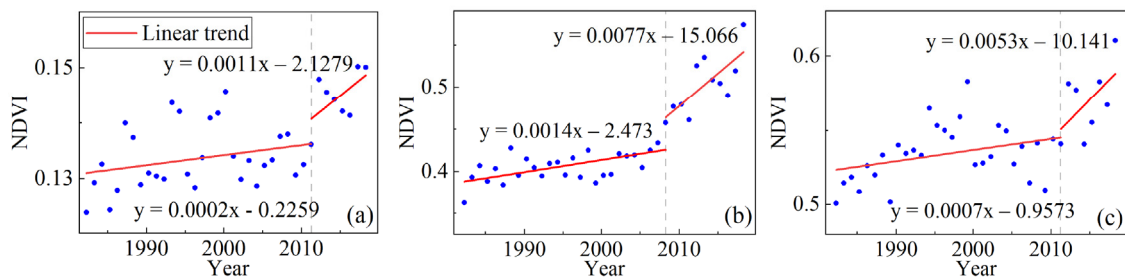
The mean NDVIs from Region I to Region III were 0.14, 0.43, and 0.54 in 1982–2018, respectively. The spatial distribution of annual mean NDVIs in the three regions is shown in Figure 3. The NDVI is low on the whole in Region I, which is dominated by very low vegetation coverage and low vegetation coverage that separately account for 69% and 23%, and other vegetation coverage areas are interlaced in the middle-upper part. High, medium, and low vegetation coverage areas are distributed from the south to north of Region II, which separately account for 29%, 52%, and 19%. Region III mainly contains medium and high vegetation coverage areas, which separately account for 31% and 60%.



**Figure 3.** Spatial distribution of annual mean NDVIs in typical ecological reserves in TNSFR from 1982 to 2018 ((a) Region I; (b) Region II; and (c) Region III).

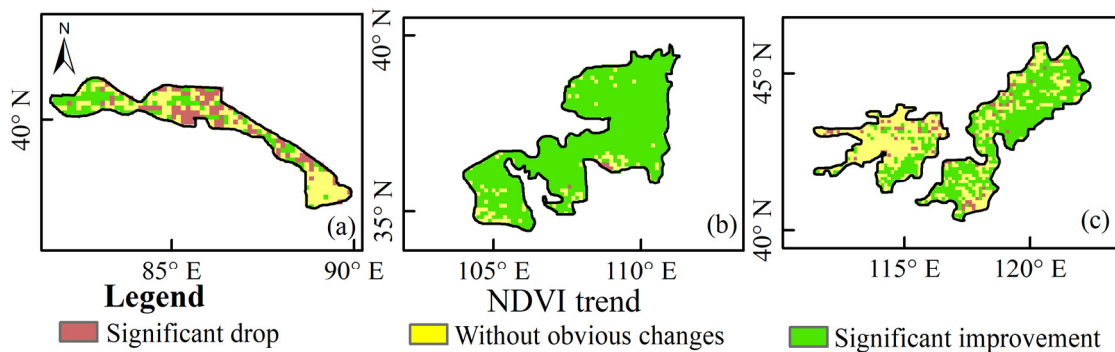
#### 3.1.2. Temporal Characteristics of NDVIs

Figure 4 shows the temporal changes in the NDVIs of the research regions. NDVIs always show an increasing trend, which indicates that vegetation coverage is improved in all three regions on the whole. The heuristic segmentation reveals that the NDVI series of the three regions changed abruptly, separately, in 2011 (Region I), 2008 (Region II), and 2011 (Region III). In the planting period of the Three-North Shelter Forest Program, the average growth rates of the NDVIs from Region I to Region III were, separately,  $2 \times 10^{-4}$ ,  $1.4 \times 10^{-3}$ , and  $7 \times 10^{-4}$ . The growth rates rose significantly after entering the tending period, and the average growth rates of the NDVIs from Region I to Region III were  $1.1 \times 10^{-3}$ ,  $7.7 \times 10^{-3}$ , and  $5.3 \times 10^{-3}$ , respectively.



**Figure 4.** NDVI time series in typical ecological reserves of TNSFR from 1982 to 2018 ((a) Region I; (b) Region II; and (c) Region III).

The linear change trend of NDVIs is calculated pixel by pixel, as displayed in Figure 5. In Region I, different types of change trends of NDVIs are spatially interlaced, and the areas with a significant drop, significant improvement, and without obvious changes account for 26%, 30%, and 44%, respectively.



**Figure 5.** Spatial distribution of change trends of NDVIs in typical ecological reserves of TNSFR from 1982 to 2018 ((a) Region I; (b) Region II; and (c) Region III).

The NDVIs in Region II exhibit a significant improvement trend on the whole, which accounts for 91%. In Region III, the changes in the NDVIs are mainly shown as a significant improvement (50%) and without obvious changes (44%). Areas with significant improvement in the NDVIs are mainly distributed in the middle and east of Region III; the west of Region III mainly covers nearly unchanged areas.

### 3.2. Relative Contributions of Climate Changes and Human Activities to Vegetation Dynamics

#### 3.2.1. Dominated Factors Causing Vegetation Restoration

The spatial distribution of the dominant driving mechanisms contributing to vegetation restoration was analyzed by combining with Figure 6. In the planting period, vegetation restoration in Regions III and I was mainly regulated by human activities, which dominated 72% of the vegetation restoration in Region I. Vegetation restoration in Region II was mainly affected by BCR and HAR. In Region III, 64% of the vegetation restoration was controlled by human activities, which were mainly concentrated in the east.

In the tending period, the impact of climate changes on vegetation restoration was enhanced in all three regions. In Region I, the proportions of CCR and BCR areas separately increased by 24% and 19%. In Region II, CCR and BCR areas collectively accounted for 80%, and except for the southeast where vegetation restoration was dominated by human activities, vegetation restoration in other areas was affected by climate changes. In Region III, the proportion of the HAR area shrank by 28%, and more vegetation restoration was impacted by climate changes.

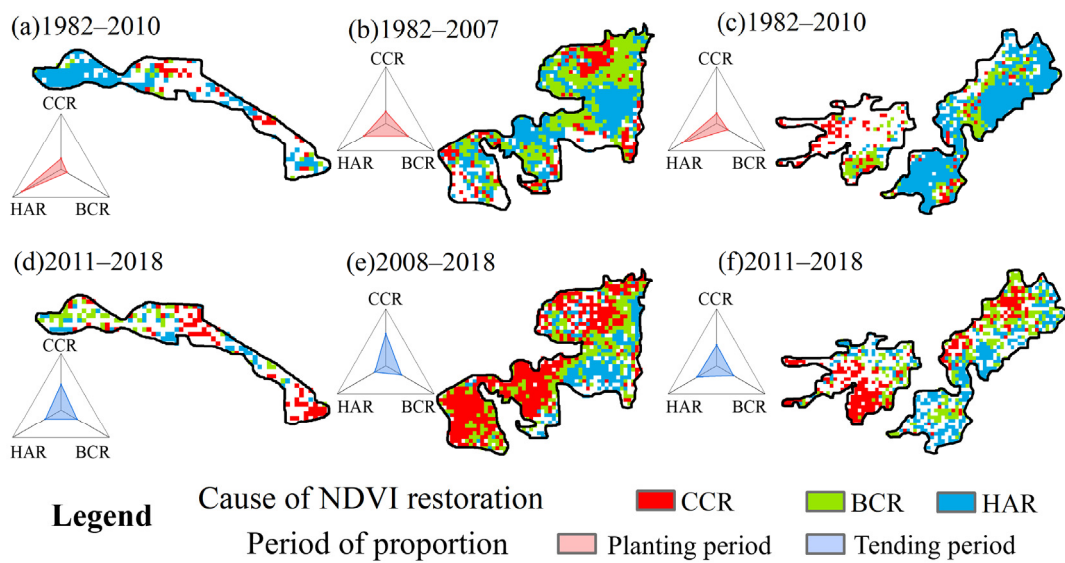


**Figure 6.** Spatial distribution of dominated driving mechanisms that cause NDVI restoration in typical ecological reserves of TNSFR in 1982–2018 and proportions of different driving mechanisms (planting period (a–c); tending period (d–f)).

### 3.2.2. Dominant Factors Causing Vegetation Degradation

Figure 7 shows the relative contributions of climate changes and human activities to vegetation degradation. In the planting period, vegetation degradation areas were concentrated. The driving mechanisms of vegetation degradation in Region I are listed in a descending order as CCD (49%), HAD (34%), and BCD (17%). In Region II, the main driving mechanism of vegetation degradation was CCD, which was mainly distributed in the south of the region. Vegetation degradation in Region III was mainly affected by human activities, in which the total proportion of HAD and BCD was 85%, and HAD was mainly concentrated in the west of the region.

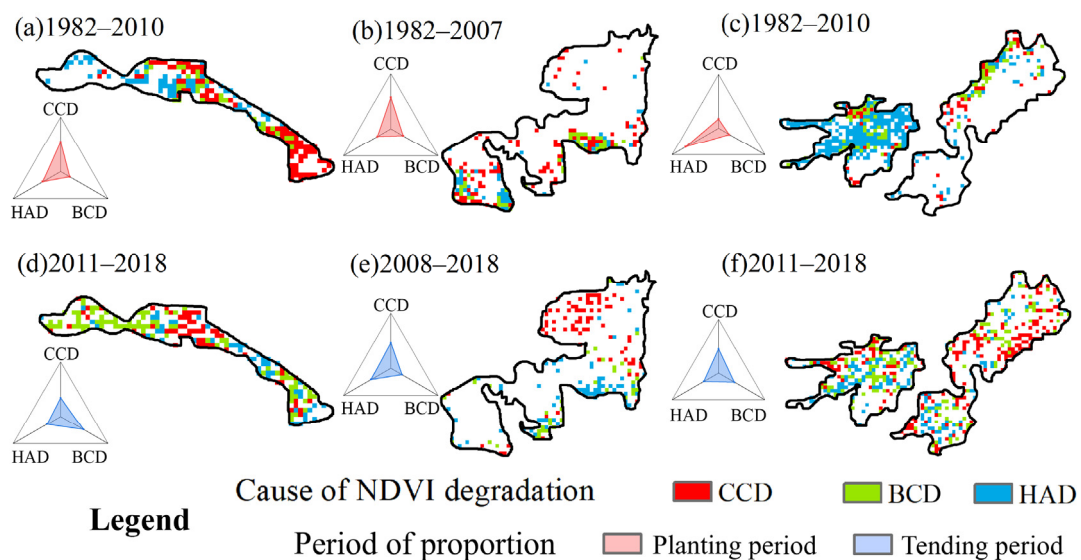


**Figure 7.** Spatial distribution of dominant driving mechanisms of NDVI degradation in typical ecological reserves of TNSFR in 1982–2018 and proportions of different driving mechanisms (planting period (a–c); tending period (d–f)).

After a year of abrupt changes, vegetation degradation spread in the space. The proportion of BCD enlarged by 26% in Region I, in which vegetation degradation areas

were interlaced with restoration areas. Vegetation degradation in the north of Region II was mainly dominated by climate changes, and areas at the southern margin were dominated by human activities. The impacts of climate changes began to be prominent in Region III. In Region III, vegetation degradation in the southwest was mainly influenced by human activities, while that in the north was mainly under the impact of climate changes.

### 3.3. Correlations of Vegetation Dynamics with Climate Changes

The partial correlation coefficients were selected to show correlations of NDVIs with temperature and precipitation in the three ecological reserves, and the spatial distribution is displayed in Figure 8. In Region I, temperature and precipitation differ slightly in the spatial distribution of correlations with NDVIs. In Region II, areas showing positive correlations between NDVIs and precipitation account for 89%, in which 42% of areas have partial correlation coefficients larger than 0.5; areas where temperature shows positive correlations with NDVIs account for 77%, in which only 17% of areas have partial correlation coefficients larger than 0.5. Region III mainly covers areas without correlations and with positive correlations between temperature and NDVIs. In Region III, the precipitation is mainly positively correlated with NDVIs and accounts for 66% and is mainly distributed in the west and northeast of the region. In summary, temperature and precipitation exert basically approximate influences on vegetation in Region I, while correlations of vegetation with precipitation are stronger than those with temperature in Regions II and III.

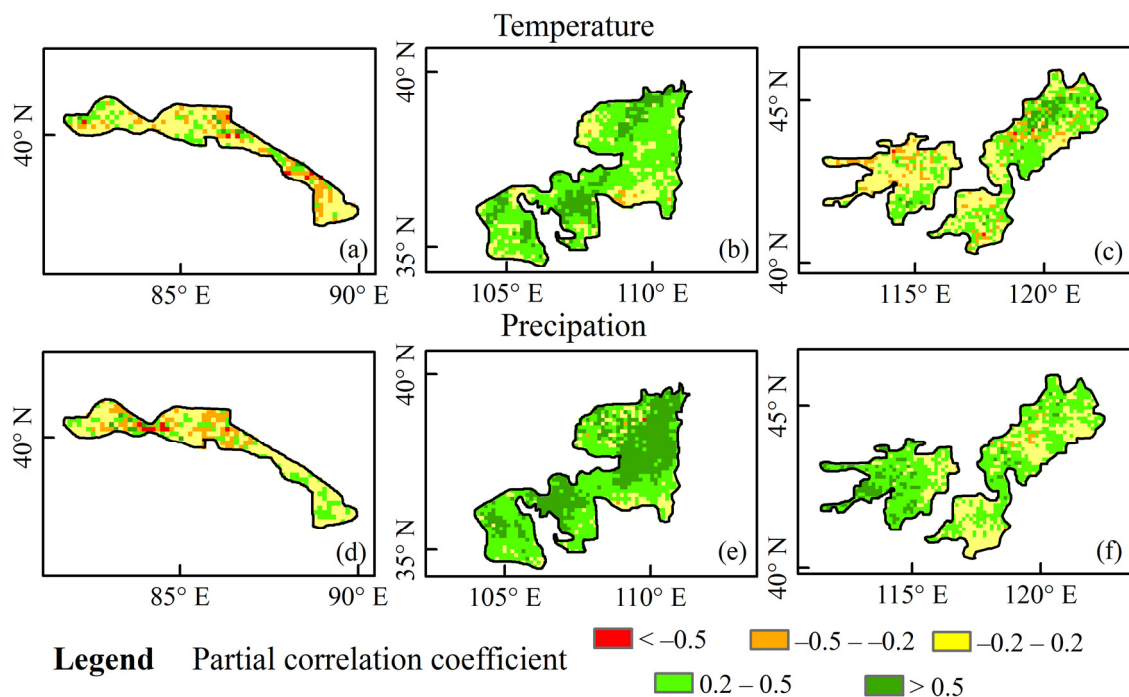


**Figure 8.** Spatial distribution of partial correlation coefficients of temperature (a–c) and precipitation (d–f) with vegetation in typical ecological reserves of TNSFR in 1982–2018.

### 3.4. Evaluation of Human Activities in Typical Ecological Reserves of TNSFR

#### 3.4.1. Human Activity Intensity

The variation in human activities in typical ecological reserves of the TNSFR is shown in Table 5. Human activity intensity gradually rose from Region I to Region III. Human activity intensity decreased at first and then increased in Region I. Regions II and III both showed enhanced human activity intensity. In Region II, the human activity intensity grew rapidly from 15.8% to 16.5% in 2010–2018. The human activity intensity rose by 0.6% in the planting period, while it increased by 0.3% in the tending period in Region III.

**Table 5.** Human activity intensity and its variation in typical ecological reserves of TNSFR.

Region	Intensity			Variation		
	1980	2010	2018	1982–2010	2010–2018	1982–2018
I	8.1	7	7.3	−1.1	0.3	−0.8
II	15.7	15.8	16.5	0.1	0.7	0.8
III	16.1	16.7	17	0.6	0.3	0.9

3.4.2. Distribution of Human Activities

Figure 9a–c illustrate the spatial distribution of human activities in each region. In Region I, human activities are mainly distributed near oases in the middle and north, while they are sparse in the south (Figure 9a). Human activities are widely distributed in Regions II and III, while the northwest of the two regions is slightly influenced by human activities (Figure 9b,c).

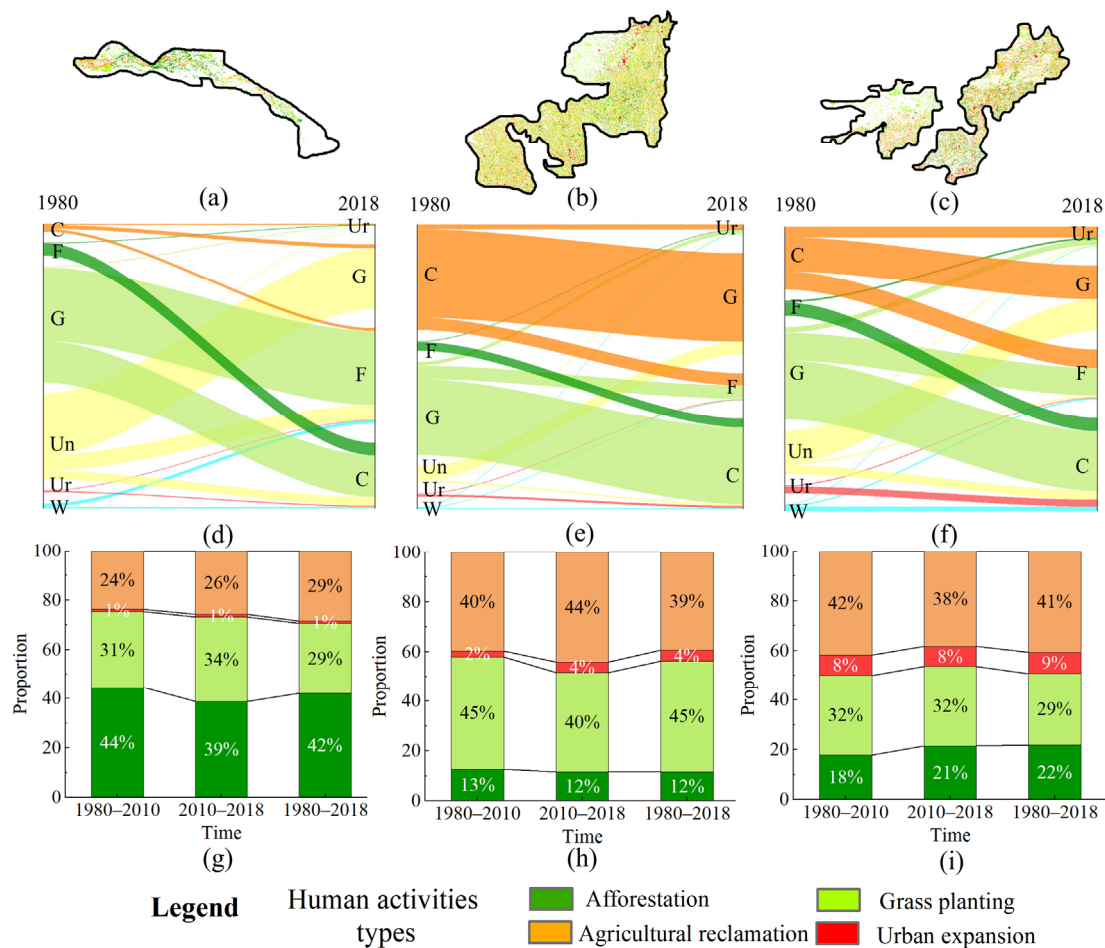


**Figure 9.** Spatial distribution of human activities in typical ecological reserves of TNSFR in 1980–2018 in Region I (a), Region II (b), and Region III (c); transition of land cover types under impacts of human activities in Region I (d), Region II (e), and Region III (f); proportions of areas with different types of human activities in Region I (g), Region II (h), and Region III (i). C (Cropland); F (Forest); G (Grassland); UN (Unused land); UR (Urban and built-up); and W (Water).

As shown in Figure 9d–i, the dynamic changes in land-use types in the three typical ecological reserves were closely related to human activities in 1982–2018. Because human activities in Region I mainly included afforestation (42%), agricultural reclamation (29%), and grass planting (29%), unused land in the region was transformed into grassland and forest, while grassland was mainly transformed into forest and cropland. Agricultural

reclamation and grass planting were the main human activities in Region II, and the two were the main sources of transformation in each other. Changes in land-use types in Region III mainly included transformation from cropland to grassland, transformation from grassland to forest, and transformation of unused land to grassland.

Ecological measures accounted for more than 50% in all 3 typical ecological reserves. Proportions of ecological measures and development activities varied slightly in different periods in Region I. After entering the tending period, the proportion of agricultural reclamation rose by 4% while that of grass planting reduced by 5% in Region II. In the tending period, the proportion of agricultural reclamation decreased by 38% while that of afforestation increased by 21% in Region III.

The comparison of the proportions of each type of human activity in different regions reveals that the proportions of development activities gradually rose to 30%, 43%, and 50% from Region I to Region III in 1980–2018, in which urban expansion accounted for 1%, 4%, and 9%.

## 4. Discussion

### 4.1. Vegetation Dynamics in Typical Ecological Reserves of TNSFR

By combining the vegetation dynamics in Figures 4 and 9, it can be seen that NDVIs mainly rose in the range of human activities in the three typical afforestation regions from 1982 to 2018, which is indicative of the restoration of vegetation in these regions. The NDVI series changed in the three regions, with abrupt changes all around 2010, which is approximate to results in other research [54–56]. In the planting period, vegetation restoration in all of the three ecological reserves is distributed within the range of human activities while accompanied by local degradation as well. After entering the tending period, vegetation restoration was still maintained in each region, and vegetation was improved with a rising rate, while the degradation also spread. This was probably caused by the death of vegetation due to factors including inappropriate vegetation types, plant diseases and insect pests, and water shortage [57–59].

### 4.2. Driving Mechanisms of Vegetation Dynamics

Figure 10 shows the proportions of different driving mechanisms (climate changes and human activities) of vegetation dynamics in different periods in each region. In the planting period, vegetation restoration in the three typical ecological reserves was dominated by human activities, and the proportions of human activities from Region I to Region III were 36%, 33%, and 41%. This is mainly related to the ecological restoration projects implemented in these regions [60,61]. After entering the tending period, the impact of human activities on vegetation restoration reduced, and the proportions of HARs, separately, decreased by 23%, 16%, and 19% in Regions I, II, and III. This is probably because the focus of ecological projects shifted from large-scale plantation to vegetation-tending [62]. In the meantime, the driving effect of climate changes on vegetation dynamics was enhanced. The proportions of the CCRs all rose, and they separately increased by 10%, 27%, and 10% from Region I to Region III, probably because of changes in the growth conditions of the vegetation due to climate changes [63,64].

### 4.3. Impact of Climate Changes on Vegetation

The research reveals that vegetation dynamics in Region I show approximate correlations with two climate factors, namely, temperature and precipitation, which is because Region I is located in the inland [65,66]. Meanwhile, because Region I is at the margin of a desert, there are large areas of regions where NDVIs are uncorrelated with the climate factors. Vegetation dynamics in Regions II and III are more closely correlated with precipitation, which is consistent with the conclusions of other research [20,67–69]. Changes in climate factors induce variation in local hydrothermal conditions and thus affect the growth process of plants [70].

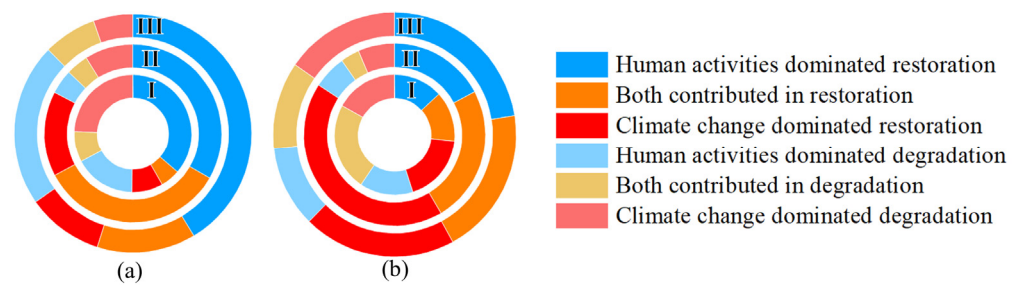


**Figure 10.** Proportions of driving mechanisms of vegetation dynamics in typical ecological reserves of TNSFR in 1980–2018 ((a) planting period; (b) tending period; I, II, and III represent the region I, II, and III, respectively).

#### 4.4. Impact of Human Activities on Vegetation

Various ecological projects implemented in the TNSFR determine the types of ecological measures, which influence the vegetation in regions by changing the land cover types [68]. The ecological projects implemented in the subregion are shown in Table 6. For the purpose of curbing desertification and protecting cropland, ecological projects in Region I are related to the forest, cropland, and grassland [2]. The main human activities in Region II pertain to cropland and grassland, which is closely related to the Restoring Cropland to Grassland Program and Cropland Protection Program implemented in the region [71]. Ecological projects in Region III mainly include the Sand Source Controls Project and Cropland Protection Program; therefore, cropland, grassland, and forest are land-use types that are heavily affected by human activities in the region.

**Table 6.** Ecological projects implemented in different ecological reserves of TNSFR and affected land cover types.

Region	TNSFP	SCCP	Ecological Projects NFPP	RCFP	SSCP	Affected Land Cover Types
I	✓	✓	✓		✓	Forest, Cropland, Grassland
II	✓	✓		✓		Cropland, Grassland
III	✓	✓		✓	✓	Forest, Cropland, Grassland

#### 4.5. Limitations and Prospects

This research investigated the driving mechanisms of vegetation dynamics in three ecological reserves of TNSFR. Although the three sub-regions were divided, the research regions still contain a large area of non-ecological engineering and increase the certainties. Therefore, they can be more finely divided according to administrative boundaries. With regard to research time periods, the research period was 1982–2018, limited by the time length of data selected. In future research, a longer time period can be adopted by prolonging the time of data, and, at the same time, more time periods can be divided to analyze the driving mechanisms of vegetation dynamics. In the analysis process of driving mechanisms, due to the specificity of each ecological reserve, the selection of the same meteorological factors may bring some uncertainties; types of human activities can be further refined to accurately identify the influences of human activities on regional vegetation dynamics.

## 5. Conclusions

The vegetation dynamics and their driving mechanisms were analyzed by using the NDVI series of the TNSFR in 1982–2018. The following conclusions are drawn:

- (1) The NDVIs in the range of human activities of the three typical ecological reserves mainly showed an increasing trend in 1982–2018, suggesting the restoration of vegetation.
- (2) In the planting period of the TNSFR, vegetation restoration in each region was mainly attributed to human activities. After a year of abrupt changes, the impact of climate changes on vegetation dynamics was enhanced in all regions.

- (3) Ecological projects in the three ecological reserves dominated the quantity of vegetation restoration, while climate changes influenced the quality of vegetation restoration. With the continuous implementation of ecological projects, the impact of climate factors on vegetation should be considered, and ecological measures need to be constantly adjusted so as to weaken the adverse effects of climate changes on vegetation and better maintain the effects of ecological projects.

**Author Contributions:** Conceptualization, Q.Q.; methodology, W.L.; software, W.L.; validation, W.L.; formal analysis, W.L.; investigation, B.W.; resources, Q.Q.; data curation, B.W.; writing—original draft preparation, W.L.; writing—review and editing, Q.Q.; visualization, W.L. and B.W.; supervision, Q.Q. and S.M.; funding acquisition, S.M. All authors have read and agreed to the published version of the manuscript.

**Funding:** This research was supported by the National Natural Science Foundation of China, grant number 52179024.

**Institutional Review Board Statement:** Not applicable.

**Informed Consent Statement:** Not applicable.

**Data Availability Statement:** MODIS datasets of MOD13A3 were obtained from <https://ladsweb.modaps.eosdis.nasa.gov/> (accessed on 15 August 2022); GIMMS datasets and meteorological data were provided by <http://data.tpdc.ac.cn/en/> (accessed on 15 August 2022); and LUCC data were obtained from <https://www.resdc.cn/> (accessed on 15 August 2022).

**Acknowledgments:** The authors are grateful to the editors and the anonymous reviewers for their insightful comments and helpful suggestions.

**Conflicts of Interest:** The authors declare no conflict of interest.

## References

- Han, Q.; Zhang, J.; Shi, X.; Zhou, D.; Ding, Y.; Peng, S. Ecological Function-Oriented Vegetation Protection and Restoration Strategies in China's Loess Plateau. *J. Environ. Manag.* **2022**, *323*, 116290. [\[CrossRef\]](#)
- Ma, S.; Wang, H.Y.; Wang, L.J.; Jiang, J.; Gong, J.W.; Wu, S.; Luo, G.Y. Evaluation and Simulation of Landscape Evolution and Its Ecological Effects under Vegetation Restoration in the Northern Sand Prevention Belt, China. *Catena* **2022**, *218*, 106555. [\[CrossRef\]](#)
- Huang, S.; Zheng, X.; Ma, L.; Wang, H.; Huang, Q.; Leng, G.; Meng, E.; Guo, Y. Quantitative Contribution of Climate Change and Human Activities to Vegetation Cover Variations Based on GA-SVM Model. *J. Hydrol.* **2020**, *584*, 124687. [\[CrossRef\]](#)
- Piao, S.; Wang, X.; Park, T.; Chen, C.; Lian, X.; He, Y.; Bjerke, J.W.; Chen, A.; Ciais, P.; Tømmervik, H.; et al. Characteristics, Drivers and Feedbacks of Global Greening. *Nat. Rev. Earth Environ.* **2020**, *1*, 14–27.
- Xu, X.; Liu, H.; Jiao, F.; Gong, H.; Lin, Z. Nonlinear Relationship of Greening and Shifts from Greening to Browning in Vegetation with Nature and Human Factors along the Silk Road Economic Belt. *Sci. Total Environ.* **2021**, *766*, 142553. [\[CrossRef\]](#)
- Piao, S.; Yin, G.; Tan, J.; Cheng, L.; Huang, M.; Li, Y.; Liu, R.; Mao, J.; Myneni, R.B.; Peng, S.; et al. Detection and Attribution of Vegetation Greening Trend in China over the Last 30 Years. *Glob. Chang. Biol.* **2015**, *21*, 1601–1609. [\[CrossRef\]](#)
- Cao, R.; Chen, Y.; Shen, M.; Chen, J.; Zhou, J.; Wang, C.; Yang, W. A Simple Method to Improve the Quality of NDVI Time-Series Data by Integrating Spatiotemporal Information with the Savitzky-Golay Filter. *Remote Sens. Environ.* **2018**, *217*, 244–257. [\[CrossRef\]](#)
- Guo, E.; Wang, Y.; Wang, C.; Sun, Z.; Bao, Y.; Mandula, N.; Jirigala, B.; Bao, Y.; Li, H. NDVI Indicates Long-Term Dynamics of Vegetation and Its Driving Forces from Climatic and Anthropogenic Factors in Mongolian Plateau. *Remote Sens.* **2021**, *13*, 688. [\[CrossRef\]](#)
- Du, J.; Quan, Z.; Fang, S.; Liu, C.; Wu, J.; Fu, Q. Spatiotemporal Changes in Vegetation Coverage and Its Causes in China since the Chinese Economic Reform. *Environ. Sci. Pollut. Res.* **2020**, *27*, 1144–1159. [\[CrossRef\]](#)
- Guan, J.; Yao, J.; Li, M.; Zheng, J. Assessing the Spatiotemporal Evolution of Anthropogenic Impacts on Remotely Sensed Vegetation Dynamics in Xinjiang, China. *Remote Sens.* **2021**, *13*, 4651. [\[CrossRef\]](#)
- Shi, S.; Yu, J.; Wang, F.; Wang, P.; Zhang, Y.; Jin, K. Quantitative Contributions of Climate Change and Human Activities to Vegetation Changes over Multiple Time Scales on the Loess Plateau. *Sci. Total Environ.* **2021**, *755*, 142419. [\[CrossRef\]](#)
- Shi, Y.; Jin, N.; Ma, X.; Wu, B.; He, Q.; Yue, C.; Yu, Q. Attribution of Climate and Human Activities to Vegetation Change in China Using Machine Learning Techniques. *Agric. For. Meteorol.* **2020**, *294*, 108146. [\[CrossRef\]](#)
- Yang, L.; Shen, F.; Zhang, L.; Cai, Y.; Yi, F.; Zhou, C. Quantifying Influences of Natural and Anthropogenic Factors on Vegetation Changes Using Structural Equation Modeling: A Case Study in Jiangsu Province, China. *J. Clean. Prod.* **2021**, *280*, 124330. [\[CrossRef\]](#)

14. Wu, J.; Li, M.; Zhang, X.; Fiedler, S.; Gao, Q.; Zhou, Y.; Cao, W.; Hassan, W.; Märgärint, M.C.; Tarolli, P.; et al. Disentangling Climatic and Anthropogenic Contributions to Nonlinear Dynamics of Alpine Grassland Productivity on the Qinghai-Tibetan Plateau. *J. Environ. Manag.* **2021**, *281*, 111875. [[CrossRef](#)]
15. Wessels, K.J.; van den Bergh, F.; Scholes, R.J. Limits to Detectability of Land Degradation by Trend Analysis of Vegetation Index Data. *Remote Sens. Environ.* **2012**, *125*, 10–22. [[CrossRef](#)]
16. Sun, L.; Zhao, D.; Zhang, G.; Wu, X.; Yang, Y.; Wang, Z. Using SPOT VEGETATION for Analyzing Dynamic Changes and Influencing Factors on Vegetation Restoration in the Three-River Headwaters Region in the Last 20 Years (2000–2019), China. *Ecol. Eng.* **2022**, *183*, 106742. [[CrossRef](#)]
17. da Rocha Miranda, J.; da Silva, R.G.; Juvanhol, R.S. Forest Fire Action on Vegetation from the Perspective of Trend Analysis in Future Climate Change Scenarios for a Brazilian Savanna Region. *Ecol. Eng.* **2022**, *175*, 106488. [[CrossRef](#)]
18. Wang, J.; Wang, K.; Zhang, M.; Zhang, C. Impacts of Climate Change and Human Activities on Vegetation Cover in Hilly Southern China. *Ecol. Eng.* **2015**, *81*, 451–461. [[CrossRef](#)]
19. Lamchin, M.; Wang, S.W.; Lim, C.H.; Ochir, A.; Pavel, U.; Gebru, B.M.; Choi, Y.; Jeon, S.W.; Lee, W.K. Understanding Global Spatio-Temporal Trends and the Relationship between Vegetation Greenness and Climate Factors by Land Cover during 1982–2014. *Glob. Ecol. Conserv.* **2020**, *24*, e01299. [[CrossRef](#)]
20. Qiu, B.; Chen, G.; Tang, Z.; Lu, D.; Wang, Z.; Chen, C. Assessing the Three-North Shelter Forest Program in China by a Novel Framework for Characterizing Vegetation Changes. *ISPRS J. Photogramm. Remote Sens.* **2017**, *133*, 75–88. [[CrossRef](#)]
21. Song, W.; Feng, Y.; Wang, Z. Ecological Restoration Programs Dominate Vegetation Greening in China. *Sci. Total Environ.* **2022**, *848*, 157729. [[CrossRef](#)]
22. Hu, Y.; Li, H.; Wu, D.; Chen, W.; Zhao, X.; Hou, M.; Li, A.; Zhu, Y. LAI-Indicated Vegetation Dynamic in Ecologically Fragile Region: A Case Study in the Three-North Shelter Forest Program Region of China. *Ecol. Indic.* **2021**, *120*, 106932. [[CrossRef](#)]
23. Xie, X.; Liang, S.; Yao, Y.; Jia, K.; Meng, S.; Li, J. Detection and Attribution of Changes in Hydrological Cycle over the Three-North Region of China: Climate Change versus Afforestation Effect. *Agric. For. Meteorol.* **2015**, *203*, 74–87. [[CrossRef](#)]
24. Peng, D.; Wu, C.; Zhang, B.; Huete, A.; Zhang, X.; Sun, R.; Lei, L.; Huang, W.; Liu, L.; Liu, X.; et al. The Influences of Drought and Land-Cover Conversion on Inter-Annual Variation of NPP in the Three-North Shelterbelt Program Zone of China Based on MODIS Data. *PLoS ONE* **2016**, *11*, e0158173. [[CrossRef](#)]
25. Cao, S.; Suo, X.; Xia, C. Payoff from Afforestation under the Three-North Shelter Forest Program. *J. Clean. Prod.* **2020**, *256*, 120461. [[CrossRef](#)]
26. Li, X.; Ning, Z.; Yang, H. A Review of the Relationship between China's Key Forestry Ecology Projects and Carbon Market under Carbon Neutrality. *Trees For. People* **2022**, *9*, 100311. [[CrossRef](#)]
27. Yang, X.; Xu, B.; Jin, Y.; Qin, Z.; Ma, H.; Li, J.; Zhao, F.; Chen, S.; Zhu, X. Remote Sensing Monitoring of Grassland Vegetation Growth in the Beijing-Tianjin Sandstorm Source Project Area from 2000 to 2010. *Ecol. Indic.* **2015**, *51*, 244–251. [[CrossRef](#)]
28. Li, W.; Wang, W.; Chen, J.; Zhang, Z. Assessing Effects of the Returning Farmland to Forest Program on Vegetation Cover Changes at Multiple Spatial Scales: The Case of Northwest Yunnan, China. *J. Environ. Manag.* **2022**, *304*, 114303. [[CrossRef](#)]
29. Zhang, Y.; Yuan, J.; You, C.; Cao, R.; Tan, B.; Li, H.; Yang, W. Contributions of National Key Forestry Ecology Projects to the Forest Vegetation Carbon Storage in China. *For. Ecol. Manag.* **2020**, *462*, 117981. [[CrossRef](#)]
30. Ibrahim, Y.Z.; Balzter, H.; Kaduk, J.; Tucker, C.J. Land Degradation Assessment Using Residual Trend Analysis of GIMMS NDVI3g, Soil Moisture and Rainfall in Sub-Saharan West Africa from 1982 to 2012. *Remote Sens.* **2015**, *7*, 5471–5494.
31. He, J.; Yang, K.; Tang, W.; Lu, H.; Qin, J.; Chen, Y.; Li, X. The First High-Resolution Meteorological Forcing Dataset for Land Process Studies over China. *Sci. Data* **2020**, *7*, 1–11. [[CrossRef](#)]
32. Yang, K.; He, J.; Tang, W.; Qin, J.; Cheng, C.C.K. On Downward Shortwave and Longwave Radiations over High Altitude Regions: Observation and Modeling in the Tibetan Plateau. *Agric. For. Meteorol.* **2010**, *150*, 38–46. [[CrossRef](#)]
33. Fensholt, R.; Proud, S.R. Evaluation of Earth Observation Based Global Long Term Vegetation Trends - Comparing GIMMS and MODIS Global NDVI Time Series. *Remote Sens. Environ.* **2012**, *119*, 131–147. [[CrossRef](#)]
34. Li, Y.; Li, Z.; Zhang, X.; Gui, J.; Xue, J. Vegetation Variations and Its Driving Factors in the Transition Zone between Tibetan Plateau and Arid Region. *Ecol. Indic.* **2022**, *141*, 109101. [[CrossRef](#)]
35. Cheng, Y.; Zhang, L.; Zhang, Z.; Li, X.; Wang, H.; Xi, X. Spatiotemporal Variation and Influence Factors of Vegetation Cover in the Yellow River Basin (1982–2021) Based on GIMMS NDVI and MOD13A1. *Water* **2022**, *14*, 3274. [[CrossRef](#)]
36. Liu, Y.; Li, Z.; Chen, Y.; Li, Y.; Li, H.; Xia, Q.; Kayumba, P.M. Evaluation of Consistency among Three NDVI Products Applied to High Mountain Asia in 2000–2015. *Remote Sens. Environ.* **2022**, *269*, 112821. [[CrossRef](#)]
37. Bernaola-Galván, P.; Ivanov, P.C.; Nunes Amaral, L.A.; Stanley, H.E. Scale Invariance in the Nonstationarity of Human Heart Rate. *Phys. Rev. Lett.* **2001**, *87*, 1–4. [[CrossRef](#)]
38. Jehanzaib, M.; Shah, S.A.; Yoo, J.; Kim, T.W. Investigating the Impacts of Climate Change and Human Activities on Hydrological Drought Using Non-Stationary Approaches. *J. Hydrol.* **2020**, *588*, 125052. [[CrossRef](#)]
39. Fokeng, R.M.; Fogwe, Z.N. Landsat NDVI-Based Vegetation Degradation Dynamics and Its Response to Rainfall Variability and Anthropogenic Stressors in Southern Bui Plateau, Cameroon. *Geosyst. Geoenviron.* **2022**, *1*, 100075. [[CrossRef](#)]
40. Evans, J.; Geerken, R. Discrimination between Climate and Human-Induced Dryland Degradation. *J. Arid Environ.* **2004**, *57*, 535–554. [[CrossRef](#)]

41. Yu, M.; Song, S.; He, G.; Shi, Y. Vegetation Landscape Changes and Driving Factors of Typical Karst Region in the Anthropocene. *Remote Sens.* **2022**, *14*, 5391. [[CrossRef](#)]
42. Teng, M.; Zeng, L.; Hu, W.; Wang, P.; Yan, Z.; He, W.; Zhang, Y.; Huang, Z.; Xiao, W. The Impacts of Climate Changes and Human Activities on Net Primary Productivity Vary across an Ecotone Zone in Northwest China. *Sci. Total Environ.* **2020**, *714*, 136691. [[CrossRef](#)] [[PubMed](#)]
43. Zhang, X.; Zhao, Y.; Ma, K.; Wang, D.; Lin, H. The Trend of Grassland Restoration and Its Driving Forces in Ningxia Hui Autonomous Region of China from 1988 to 2018. *Sustainability* **2022**, *14*, 10404. [[CrossRef](#)]
44. Zhou, W.; Gang, C.; Zhou, F.; Li, J.; Dong, X.; Zhao, C. Quantitative Assessment of the Individual Contribution of Climate and Human Factors to Desertification in Northwest China Using Net Primary Productivity as an Indicator. *Ecol. Indic.* **2015**, *48*, 560–569. [[CrossRef](#)]
45. Li, Y.; Zhao, Z.; Wang, L.; Li, G.; Chang, L.; Li, Y. Vegetation Changes in Response to Climatic Factors and Human Activities in Jilin Province, China, 2000–2019. *Sustainability* **2021**, *13*, 8956. [[CrossRef](#)]
46. Naeem, S.; Zhang, Y.; Zhang, X.; Tian, J.; Abbas, S.; Luo, L.; Meresa, H.K. Both Climate and Socioeconomic Drivers Contribute to Vegetation Greening of the Loess Plateau. *Sci. Bull.* **2021**, *66*, 1160–1163. [[CrossRef](#)] [[PubMed](#)]
47. Gu, Y.; Pang, B.; Qiao, X.; Xu, D.; Li, W.; Yan, Y.; Dou, H.; Ao, W.; Wang, W.; Zou, C.; et al. Vegetation Dynamics in Response to Climate Change and Human Activities in the Hulun Lake Basin from 1981 to 2019. *Ecol. Indic.* **2022**, *136*, 108700. [[CrossRef](#)]
48. Liu, H.; Deng, Y.; Liu, X. The Contribution of Forest and Grassland Change Was Greater than That of Cropland in Human-Induced Vegetation Greening in China, Especially in Regions with High Climate Variability. *Sci. Total Environ.* **2021**, *792*, 148408. [[CrossRef](#)]
49. Han, J.C.; Huang, Y.; Zhang, H.; Wu, X. Characterization of Elevation and Land Cover Dependent Trends of NDVI Variations in the Hexi Region, Northwest China. *J. Environ. Manag.* **2019**, *232*, 1037–1048. [[CrossRef](#)]
50. Xu, Y.; Xu, X.; Tang, Q. Human Activity Intensity of Land Surface: Concept, Methods and Application in China. *J. Geogr. Sci.* **2016**, *26*, 1349–1361. [[CrossRef](#)]
51. Ding, Z.; Zheng, H.; Li, H.; Yu, P.; Man, W.; Liu, M.; Tang, X.; Liu, Y. Afforestation-Driven Increases in Terrestrial Gross Primary Productivity Are Partly Offset by Urban Expansion in Southwest China. *Ecol. Indic.* **2021**, *127*. [[CrossRef](#)]
52. Shi, G.; Jiang, N.; Yao, L. Land Use and Cover Change during the Rapid Economic Growth Period from 1990 to 2010: A Case Study of Shanghai. *Sustain.* **2018**, *10*, 426. [[CrossRef](#)]
53. Chang, X.; Xing, Y.; Wang, J.; Yang, H.; Gong, W. Effects of Land Use and Cover Change (LUCC) on Terrestrial Carbon Stocks in China between 2000 and 2018. *Resour. Conserv. Recycl.* **2022**, *182*, 106333. [[CrossRef](#)]
54. Ma, D.; Yin, Y.; Wu, S.; Zheng, D. Sensitivity of Arid/Humid Patterns in China to Future Climate Change under High Emission Scenario. *Dili Xuebao/Acta Geogr. Sin.* **2019**, *74*, 857–874. [[CrossRef](#)]
55. Wang, S.; Li, R.; Wu, Y.; Zhao, S. Effects of Multi-Temporal Scale Drought on Vegetation Dynamics in Inner Mongolia from 1982 to 2015, China. *Ecol. Indic.* **2022**, *136*, 108666. [[CrossRef](#)]
56. Gao, W.; Zheng, C.; Liu, X.; Lu, Y.; Chen, Y.; Wei, Y.; Ma, Y. NDVI-Based Vegetation Dynamics and Their Responses to Climate Change and Human Activities from 1982 to 2020: A Case Study in the Mu Us Sandy Land, China. *Ecol. Indic.* **2022**, *137*, 108745. [[CrossRef](#)]
57. Duan, Z.; Xiao, H.; Li, X.; Dong, Z.; Wang, G. Evolution of Soil Properties on Stabilized Sands in the Tengger Desert, China. *Geomorphology* **2004**, *59*, 237–246. [[CrossRef](#)]
58. Wang, X.M.; Zhang, C.X.; Hasi, E.; Dong, Z.B. Has the Three Norths Forest Shelterbelt Program Solved the Desertification and Dust Storm Problems in Arid and Semiarid China? *J. Arid Environ.* **2010**, *74*, 13–22. [[CrossRef](#)]
59. Lu, W.; Hu, M.; Hu, J.; Yao, X. Discussion on Severity and Control of Asian Longhorned Beetle (ALB) of Poplar Trees in the Three North Protection Forest Program. *Prot. For. Sci. Technol.* **2004**, *1*. (In Chinese) [[CrossRef](#)]
60. Liu, Z.; Liu, Y.; Li, Y. Anthropogenic Contributions Dominate Trends of Vegetation Cover Change over the Farming–Pastoral Ecotone of Northern China. *Ecol. Indic.* **2018**, *95*, 370–378. [[CrossRef](#)]
61. Lin, M.; Hou, L.; Qi, Z.; Wan, L. Impacts of Climate Change and Human Activities on Vegetation NDVI in China’s Mu Us Sandy Land during 2000–2019. *Ecol. Indic.* **2022**, *142*, 109164. [[CrossRef](#)]
62. Zheng, X.; Zhu, J.J.; Yan, Q.L.; Song, L.N. Effects of Land Use Changes on the Groundwater Table and the Decline of *Pinus Sylvestris* Var. *Mongolica* Plantations in Southern Horqin Sandy Land, Northeast China. *Agric. Water Manag.* **2012**, *109*, 94–106. [[CrossRef](#)]
63. Chen, Z.; Liu, J.; Li, L.; Wu, Y.; Feng, G.; Qian, Z.; Sun, G.Q. Effects of Climate Change on Vegetation Patterns in Hulun Buir Grassland. *Phys. A Stat. Mech. Its Appl.* **2022**, *597*, 1–12. [[CrossRef](#)]
64. Han, Z.; Song, W. Interannual Trends of Vegetation and Responses to Climate Change and Human Activities in the Great Mekong Subregion. *Glob. Ecol. Conserv.* **2022**, *38*, e02215. [[CrossRef](#)]
65. Duan, H.; Zhao, H.; Jiang, Y.; Li, Y. Analysis of Seasonal Grassland Change and Its Drivers during 1982–2006 in Xinjiang. *Rangel. Ecol. Manag.* **2017**, *70*, 422–429. [[CrossRef](#)]
66. Zhang, Q.; Sun, C.; Chen, Y.; Chen, W.; Xiang, Y.; Li, J.; Liu, Y. Recent Oasis Dynamics and Ecological Security in the Tarim River Basin, Central Asia. *Sustainability* **2022**, *14*, 3372. [[CrossRef](#)]
67. Wang, H.; Yan, S.; Liang, Z.; Jiao, K.; Li, D.; Wei, F.; Li, S. Strength of Association between Vegetation Greenness and Its Drivers across China between 1982 and 2015: Regional Differences and Temporal Variations. *Ecol. Indic.* **2021**, *128*, 107831. [[CrossRef](#)]

68. Yu, L.; Wu, Z.; Du, Z.; Zhang, H.; Liu, Y. Insights on the Roles of Climate and Human Activities to Vegetation Degradation and Restoration in Beijing-Tianjin Sandstorm Source Region. *Ecol. Eng.* **2021**, *159*, 1–11. [[CrossRef](#)]
69. Li, C.; Li, X.; Luo, D.; He, Y.; Chen, F.; Zhang, B.; Qin, Q. Spatiotemporal Pattern of Vegetation Ecology Quality and Its Response to Climate Change between 2000–2017 in China. *Sustainability* **2021**, *13*, 1419. [[CrossRef](#)]
70. Du, J.; Shu, J.; Yin, J.; Yuan, X.; Jiaerheng, A.; Xiong, S.; He, P.; Liu, W. Analysis on Spatio-Temporal Trends and Drivers in Vegetation Growth during Recent Decades in Xinjiang, China. *Int. J. Appl. Earth Obs. Geoinf.* **2015**, *38*, 216–228. [[CrossRef](#)]
71. Wu, X.; Wang, S.; Fu, B.; Liu, J. Spatial Variation and Influencing Factors of the Effectiveness of Afforestation in China's Loess Plateau. *Sci. Total Environ.* **2021**, *771*, 144904. [[CrossRef](#)] [[PubMed](#)]

**Disclaimer/Publisher's Note:** The statements, opinions and data contained in all publications are solely those of the individual author(s) and contributor(s) and not of MDPI and/or the editor(s). MDPI and/or the editor(s) disclaim responsibility for any injury to people or property resulting from any ideas, methods, instructions or products referred to in the content.